



ELSEVIER

Contents lists available at ScienceDirect

Acta Biomaterialia

journal homepage: [www.elsevier.com/locate/actabiomat](http://www.elsevier.com/locate/actabiomat)

Full length article

# Augmented liver targeting of exosomes by surface modification with cationized pullulan

Ryo Tamura<sup>a,b</sup>, Shinji Uemoto<sup>a</sup>, Yasuhiko Tabata<sup>b,\*</sup><sup>a</sup> Department of Surgery, Graduate School of Medicine, Kyoto University, Japan<sup>b</sup> Department of Biomaterials, Institute for Frontier Medical Sciences, Kyoto University, Japan

## ARTICLE INFO

## Article history:

Received 23 January 2017

Received in revised form 27 April 2017

Accepted 4 May 2017

Available online 5 May 2017

## Keywords:

Exosome

Pullulan

Concanavalin A

Liver targeting

Nanoparticle

## ABSTRACT

Exosomes are membrane nanoparticles containing biological substances that are employed as therapeutics in experimental inflammatory models. Surface modification of exosomes for better tissue targetability and enhancement of their therapeutic ability was recently attempted mainly using gene transfection techniques. Here, we show for the first time that the surface modification of exosomes with cationized pullulan, which has the ability to target hepatocyte asialoglycoprotein receptors, can target injured liver and enhance the therapeutic effect of exosomes. Surface modification can be achieved by a simple mixing of original exosomes and cationized pullulan and through an electrostatic interaction of both substances. The exosomes modified with cationized pullulan were internalized into HepG2 cells *in vitro* to a significantly greater extent than unmodified ones and this internalization was induced through the asialoglycoprotein receptor that was specifically expressed on HepG2 cells and hepatocytes. When injected intravenously into mice with concanavalin A-induced liver injury, the modified exosomes accumulated in the liver tissue, resulting in an enhanced anti-inflammatory effect *in vivo*. It is concluded that the surface modification with cationized pullulan promoted accumulation of the exosomes in the liver and the subsequent biological function, resulting in a greater therapeutic effect on liver injury.

## Statement of significance

Exosomes have shown potentials as therapeutics for various inflammatory disease models. This study is the first to show the specific accumulation of exosomes in the liver and enhanced anti-inflammatory effect via the surface modification of exosomes using pullulan, which is specifically recognized by the asialoglycoprotein receptor (AGPR) on HepG2 cells and hepatocytes. The pullulan was expressed on the surface of PKH-labeled exosomes, and it led increased accumulation of PKH into HepG2 cells, whereas the accumulation was canceled by AGPR inhibitor. In the mouse liver injury model, the modification of PKH-labeled exosomes with pullulan enabled increased accumulation of PKH specifically in the injured liver. Furthermore the greater therapeutic effects against the liver injury compared with unmodified original exosomes was observed.

© 2017 Acta Materialia Inc. Published by Elsevier Ltd. All rights reserved.

## 1. Introduction

Exosomes are defined as membrane nanoparticles released via the fusion of multivesicular bodies with the plasma membrane [1]. They contain various biologically active substances and play an important role in intercellular communication [2,3]. A representative example of these factors is paracrine factors secreted from mesenchymal stem cells (MSCs). Studies on several animal models

have reported that the exosomal fraction present in conditioned medium of MSCs culture has therapeutic effects [2,4–6]. This unique property has encouraged the application of exosomes as therapeutic molecules [7–9]. Furthermore, an approach to modify the surface of exosomes for better tissue targetability and efficient delivery of their contents into the cytosol has recently been reported, which would be particularly promising when used in combination with genetic engineering [10–12].

The objective of this study is specific delivery of MSC-derived exosomes into the liver after their injection. It has been reported that they are internalized by macrophages after their injection and then express their effects through the immunological function

\* Corresponding author.

E-mail address: [yasuhiko@frontier.kyoto-u.ac.jp](mailto:yasuhiko@frontier.kyoto-u.ac.jp) (Y. Tabata).

of macrophages [13–15]. If MSC-derived exosomes readily accumulate in injured liver and are internalized by cells other than macrophages, they could exert their effects more directly on the tissue, conferring greater potential for therapeutic and diagnostic purposes [14].

Pullulan is a maltotriose consisting of three glucose moieties that are connected by an  $\alpha$ -1,4 glycosidic bond [16,17]. It is specifically internalized by HepG2 cells and hepatocytes through an asialoglycoprotein receptor (ASGPR) and is an efficient carrier of siRNA for specific delivery to hepatocytes [18,19]. In a previous study, modification with pullulan enabled the efficient accumulation of drugs in parenchymal hepatocytes and consequently enhanced their therapeutic effect in the liver [17].

Building on this previous work, in this study, exosomes were modified with pullulan by simple mixing to enhance their liver accumulation and therapeutic effect on a liver injury. Pullulan was cationized with spermine, a polyamine present in the body, to enhance its electrostatic interaction with the negatively charged surface of original exosomes [20]. The enhanced internalization of exosomes modified with cationized pullulan and its pathway was evaluated in an *in vitro* study, and the enhanced accumulation and therapeutic effect were confirmed *in vivo* in a concanavalin A-induced liver injury model, established as described previously [21]. The therapeutic effect of the modified exosomes and the underlying mechanisms were evaluated by histological and immunological analyses.

## 2. Materials and methods

### 2.1. Animals

All animal experiments were carried out in accordance with procedures approved by the Animal Experimentation Committee of the Institute for Frontier Medical Sciences (approval number: #F173). Male C57B6 mice were obtained from Shimizu Laboratory Supplies Co., Ltd. (Kyoto, Japan). All mice were maintained under specific pathogen-free conditions in the animal facility at the Institute for Frontier Medical Sciences.

### 2.2. Collection of exosomes

Exosomes were purified from the supernatant of MSCs culture. Collection was carried out by a slightly modified version of a previously reported procedure (Fig. 1a) [22,23]. The supernatant was centrifuged twice at 2000g and 10,000g to exclude cellular or other debris. The final supernatant was then passed through 0.45- $\mu$ m pore filters (Merck Millipore, Billerica, MA, USA) and the filtrate was used for the collection of exosomes. The exosome fraction in the filtrate was pelleted by ultracentrifugation at 100,000g for 60 min with a Hitachi CP80WX ultracentrifuge (Hitachi Koki Co., Ltd., Tokyo, Japan). The pellet was resuspended in PBS and similarly ultracentrifuged again. Collected exosomes were dispersed in phosphate-buffered saline (PBS) and the amount of exosomes collected was determined by measuring the protein concentration using the BCA Assay Kit (Thermo Fisher Scientific, Waltham, MA, USA), in accordance with the manufacturer's protocol [22]. Ultracentrifuge tubes and collection bottles for exosomes were sterilized prior to use, and the collection was carried out in a sterilized manner. Collected exosomes were stored in the refrigerator at 4 °C for up to a week before used for experiments.

### 2.3. Analyses of the size and zeta potential of collected exosomes

The diameter of collected exosomes dispersed in PBS was determined using the qNano system (Izon, Christchurch, New Zealand). Changes in the diameter and zeta potential of exosomes modified

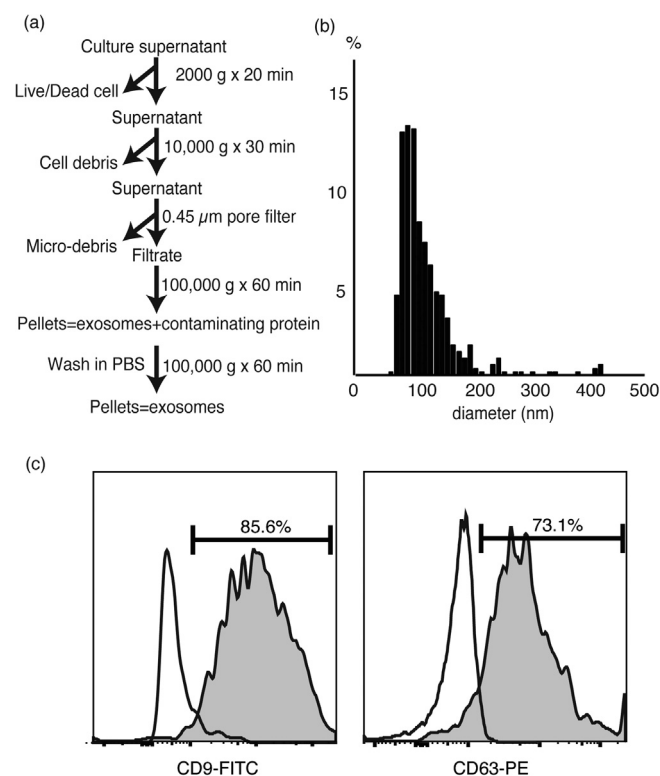


**Fig. 1.** Collection and characteristics of exosomes. (a) An overview of the collection procedure. Collected exosomes were evaluated for their diameter (b), and the fraction of typical surface markers of exosomes, CD9 and CD63, by flowcytometric analysis (c).

with pullulan into which spermine had been introduced at 6.0, 11.6, and 17.0 mol% were measured with a Zetasizer Nano ZS with He-Ne laser 633 nm wavelength (Malvern Instruments, Malvern, UK) at 20 °C. This measurement was repeated 100 times for each sample and the result is expressed as the mean. The experiment was repeated three times.

### 2.4. Preparation of cationized pullulan derivatives and their reactions with collected exosomes

Pullulan with a weight-average molecular weight of 47,300 (Hayashibara, Okayama, Japan) and spermine (Sigma Chemical, St. Louis, MO, USA) were used for a preparation of cationized pullulan. Spermine was introduced to the hydroxyl groups of pullulan by an *N,N'*-carbonyldiimidazole (CDI) activation method [18,24]. Spermine and CDI were added to 50 ml of dehydrated dimethyl sulfoxide containing 50 mg of pullulan. Following agitation using a magnetic stirrer at 35 °C for 20 h, the reaction mixture was dialyzed against ultrapure double-distilled water for 2 days using a dialysis membrane with a molecular weight cut-off of 12,000–14,000 (Viskase Companies Inc., Willowbrook, IL, USA). Then, the dialyzed solution was freeze-dried to obtain samples of cationized pullulan. The rate of spermine introduction was determined by conventional elemental analysis and expressed by the molar percentage of spermine introduced onto the hydroxyl groups of pullulan. Collected exosomes were mixed with the cationized pullulan, followed by leaving the mixed solution for 15 min at room temperature.

### 2.5. Detection of cationized pullulan on the surface of modified exosomes

The presence of cationized pullulan on the surface of exosomes was evaluated by the lectin-induced aggregation method [25,26]. A

suspension of *Ricinus communis* agglutinin of lectins recognizable by galactose (RCA120) (Vector Laboratories, Burlingame, CA, USA) in PBS at a concentration of 50 µg/100 µl was mixed with the same amount of PBS solution containing 10 µg of exosomes modified with 1 or 2 µg of pullulan into which spermine had been introduced at a rate of 6.0 mol%. Aggregation was detected as a change of turbidity measured at a wavelength of 500 nm at room temperature. To confirm the specificity of lectin–sugar interaction, D-galactose was added 40 min after the RCA120 addition. The results are expressed as the proportion of the solution absorbance to that of exosomes alone with RCA120. The experiment was repeated three times.

## 2.6. Flow cytometric analysis

The primary and secondary antibodies used in this study are shown in Table 1. Flow cytometric analysis was carried out in accordance with a previous study with FACS CANTO II using FACS Diva software (BD Bioscience, Franklin Lakes, NJ, USA) [27,28]. In brief, MSCs or liver nonparenchymal cells (NPCs) ( $1 \times 10^6$ ) were employed for each single staining. MSCs were detached from the culture dish by treatment with 0.25 wt% trypsin/1 mM EDTA for 5 min and centrifuged at 1700g for 5 min at 4 °C. After adding 50 µl of flow cytometry buffer to the cell pellet, each sample was incubated with 1 µg of anti-CD16/32 mAb at 4 °C. MSCs ( $1 \times 10^6$ ) were labeled with 1 µg of the mAbs shown in Table 1. After 30 min of incubation of cells with each mAb at 4 °C, the buffer was added to each tube and centrifuged at 1700g for 5 min at 4 °C. The cells were washed again and resuspended in 500 µl of FACS buffer consisted of PBS containing 0.2 vol% of FBS and 0.05 wt% of sodium azide. Each sample suspension was transferred to a test tube through a 200-µm pore mesh and analyzed.

For the detection of CD4-, CD25-, and FoxP3-positive regulatory T cells (Tregs) of NPCs, the anti-mouse/rat FoxP3 Staining Set (eBioscience, San Diego, CA, USA) was used, in accordance with the manufacturer's protocol.

Flowcytometric analysis of exosomes collected were carried out with reference to the previous report with some modification [22,28]. In brief, 10 µg of exosomes collected was mixed with 20 µl of aldehyde/sulfate beads (4 µm in diameter, Life technologies, Carlsbad, CA, USA). The beads reacted with exosomes was then washed with FACS buffer. The beads was incubated with FITC-labeled anti-CD9 or PE-labeled anti-CD63 and then analyzed.

## 2.7. Fluorescent labeling of exosomes with PKH26

Fluorescent labeling of collected exosomes was carried out in accordance with a previously reported procedure and unconjugated fluorescent dye was washed out by centrifugation with Amicon® Ultra 0.5 ml 30 K Centrifugal Filters (Merck Millipore) [29]. In brief, 100 µg of exosomes were dispersed in 1 ml of Diluent C of the PKH26 staining kit (Sigma-Aldrich, St. Louis, MO, USA). The solution was mixed with 4 µl of PKH26 fluorescent dye in 1 ml of Diluent C. Unconjugated fluorescent dye was washed out by centrifugation with Amicon® Ultra 0.5 ml 30 K Centrifugal Filters (Merck Millipore).

## 2.8. In vitro internalization of exosomes

HepG2 cells were employed in an *in vitro* study of the internalization of exosomes unmodified or modified with cationized pullulan. HepG2 cells were seeded in 1 ml of RPMI1640 medium (Gibco by Life Technologies, Grand Island, NY, USA) with 10 vol% fetal bovine serum and 1 vol% of penicillin and streptomycin at  $1.25 \times 10^5$  cells/cm<sup>2</sup>. The next day, 5 µg of PKH-labeled exosomes unmodified or modified with 0.5 or 1 µg of pullulan into which 6.0, 11.6, and 17.0 mol% of spermine had been introduced in 50 µl of PBS were added. The images of HepG2 cells were randomly taken with a Keyence BZ-X710 fluorescent microscope (Keyence Co., Osaka, Japan) after 0.5, 1, and 3 h of incubation. The number of PKH spots in the images was counted in an automated manner with Keyence BZ-X analyzer software (Keyence Co.) for the images of all treatment groups. Sites with a homogeneous HepG2 cell distribution were used for counting to exclude the effect of a difference in the cell number between the images. The increase in the number of PKH spots at each time point relative to that at 0.5 h was calculated. The experiment was independently repeated three times. The internalization of PKH after 3 h of incubation was visualized by the counterstaining of HepG2 cells with CellTrace CFSE (Thermo Fisher Scientific) and 0.1 vol% 4',6-diamidino-2-phenylindole dihydrochloride (DAPI) (Thermo Fisher Scientific) for the cytoplasm and nucleus, respectively. Pretreatment of HepG2 cells with asialofetuin, a competitive inhibitor of ASGPR, was carried out with reference to a previous report [19]. Subsequent imaging and counting of PKH spots were carried out in the same manner, the results of which are shown as the number of PKH spots counted.

**Table 1**  
Antibodies used in flow cytometry or immunofluorescence study.

Antibody	Source	Catalogue #	Clone
Anti-CD16/32	Biolegend (San Diego, CA, USA)	1013009	93
FITC-labeled anti-CD3	Biolegend	B134497	17A2
FITC-labeled anti-CD9	eBioscience	11-0091-81	KMC8
FITC-labeled anti-CD31	Biolegend	B112061	MEC13.3
FITC-labeled anti-FoxP3	eBioscience	11-5775-80	FJK-16s
PE-labeled anti-CD25	eBioscience	12-0251-81	PC61.5
PE-labeled anti-CD44	BD Bioscience	553134	IM7
PE-labeled anti-CD63	Cosmo Bio Co. (Tokyo, Japan)	143904	NVG-2
PE-Cy5-labeled anti-Sca1	eBioscience	25-5981-82	D7
PerCP-labeled anti-B220	Biolegend	103234	RA3-6B2
eFluor®660-labeled anti-CD34	eBioscience	560238	RAM34
APC-eFluor®780-labeled anti-CD45	eBioscience	47-0451-82	30-F11
PE-Cy7-labeled anti-CD4	BD Bioscience	552775	RM4-5
Purified anti-F4/80	Biolegend	123109	BM8
Purified anti-CD81	eBioscience	14-0811-81	EAT2
Alexa Fluor 647 Goat Anti-Rat IgG	Thermo Fisher Scientific	A21247	
Alexa-Fluor 647 Goat Anti-Hamster IgG	Thermo Fisher Scientific	A21451	

### 2.9. *In vivo* accumulation and effect of exosomes unmodified or modified with cationized pullulan

Three C57B6 male mice were employed for each treatment group in the *in vivo* study on the treatment of concanavalin A-induced liver injury. For *in vivo* tracing study of exosomes labeled with PKH, six mice were divided into two experimental groups. The mouse liver injury model was prepared by the injection of concanavalin A (Cosmo Bio Co., Ltd.) in PBS (15 mg/kg body weight) via a mouse tail vein. Immediately after the injection, 100  $\mu$ l of PBS, PBS containing 1  $\mu$ g of cationized pullulan into which spermine had been introduced at a rate of 6.0 mol%, or PBS containing 10  $\mu$ g of exosomes unmodified or modified with 1  $\mu$ g of cationized pullulan was injected through a mouse tail vein.

### 2.10. Plasma alanine aminotransferase (ALT) analysis and histopathological examination of liver in an *in vivo* study

Twenty-four hours after the injection, mice were sacrificed by cervical dislocation, samples were collected, and further analyses were carried out. For the tracing study, mice were sacrificed 4 h after the injection. Plasma ALT level was measured using a standard clinical automatic analyzer. Liver samples were frozen in liquid nitrogen for mRNA detection by reverse transcription (RT)-PCR. Hematoxylin-eosin staining and Ki-67 staining were carried out by a standard protocol with a tissue specimen fixed in 10% buffered formalin (Mildform<sup>®</sup> 10 N; Wako Pure Chemical Industries Ltd., Osaka, Japan) overnight and subsequently embedded in paraffin. Immunofluorescent staining and observation of exosomes stained with PKH26 in the liver were carried out for frozen sections prepared in accordance with a previous report [15]. Each histopathological sample was randomly observed using a Keyence BZ-X710 fluorescent microscope and the resultant images were used for analysis. For the study of liver necrotic areas, a section of the liver specimen stained with hematoxylin eosin was selected at random for visualization using the microscope and the ratio of necrotic area to liver parenchyma was calculated. To determine the Ki-67 index, images were captured in the same manner as for liver necrotic areas, and the detection and calculation of the Ki-67 index were carried out using Keyence BZ-X analyzer software in an automated manner. To analyze immunohistochemical staining, primary antibody and secondary antibody shown in Table 1 at 0.1 vol% were incubated overnight at 4 °C and for 1 h at room temperature, respectively. The nucleus was counterstained with DAPI.

### 2.11. Evaluation of the mRNA expression of inflammatory cytokines in *in vivo* study

Total RNA was purified from liver tissue using TRIzol<sup>®</sup> Reagent (Thermo Fisher Scientific), in accordance with the manufacturer's protocol. Complementary DNA (cDNA) was generated from 1  $\mu$ g of whole RNA purified using a SuperScript VILO cDNA synthesis

kit (Thermo Fisher Scientific), while the sequential analysis of cDNA was carried out by the Power SYBR<sup>®</sup> Green quantitative fluorescent PCR method (Thermo Fisher Scientific) with an Applied Biosystems 7500 Real-time PCR system (Applied Biosystems, Foster City, CA, USA). The primers used are summarized in Table 2. The PCR conditions were as follows: 95 °C for 10 min, followed by 40 cycles of 94 °C for 15 s and 60 °C for 30 s. Glyceraldehyde-3-phosphate dehydrogenase (GAPDH) was used as a housekeeping gene. Fold induction was calculated using the Ct method,  $\Delta\Delta Ct = (Ct^{\text{target}} - Ct^{\text{housekeeping}})^{\text{infected}} - (Ct^{\text{target}} - Ct^{\text{housekeeping}})^{\text{uninfected}}$ , and the final data were derived from  $2^{-\Delta\Delta Ct}$ .

### 2.12. Collection of NPCs from mouse liver samples

The isolation of NPCs was carried out in accordance with a previous report using the following reagents: collagenase D (Roche, Switzerland), HBSS (Invitrogen, Grand Island, NY, USA), RPMI1640 (Gibco by Life Technologies), and OptiPrep (Sigma-Aldrich) [27].

### 2.13. Statistical analysis

The data are presented as mean  $\pm$  standard error of the mean (SEM). Comparisons between two groups were carried out using two-tailed Student's *t* test. Differences were considered significant at  $P < 0.05$ .

## 3. Results

### 3.1. Characterization of collected exosomes and their parental MSCs

Fig. 1 shows the procedures for the collection (Fig. 1a). The mode, mean, and standard deviation of diameter of the collected exosomes were 100, 125, and 52 nm, respectively (Fig. 1b). The positive fraction of surface markers of exosomes such as CD9 or CD63 was confirmed by flowcytometric analysis (Fig. 1c).

Supplementary Fig. S1a shows the results of immunohistochemical staining of maternal MSCs that indicates their ability to undergo adipogenic, osteogenic, and chondrogenic differentiation. MSCs passaged three times expressed the MSC antigens CD44 and Sca1, as determined by flow cytometric analysis, whereas endothelial, myeloid, hematopoietic, and lymphocyte cell lineage-specific antigens such as CD31, CD34, CD45, CD3, and B220 were scarcely detected (Fig. S1b).

Typical morphology of exosomes was confirmed by TEM observation as a single particle or multiple particles (Fig. S2 left and right).

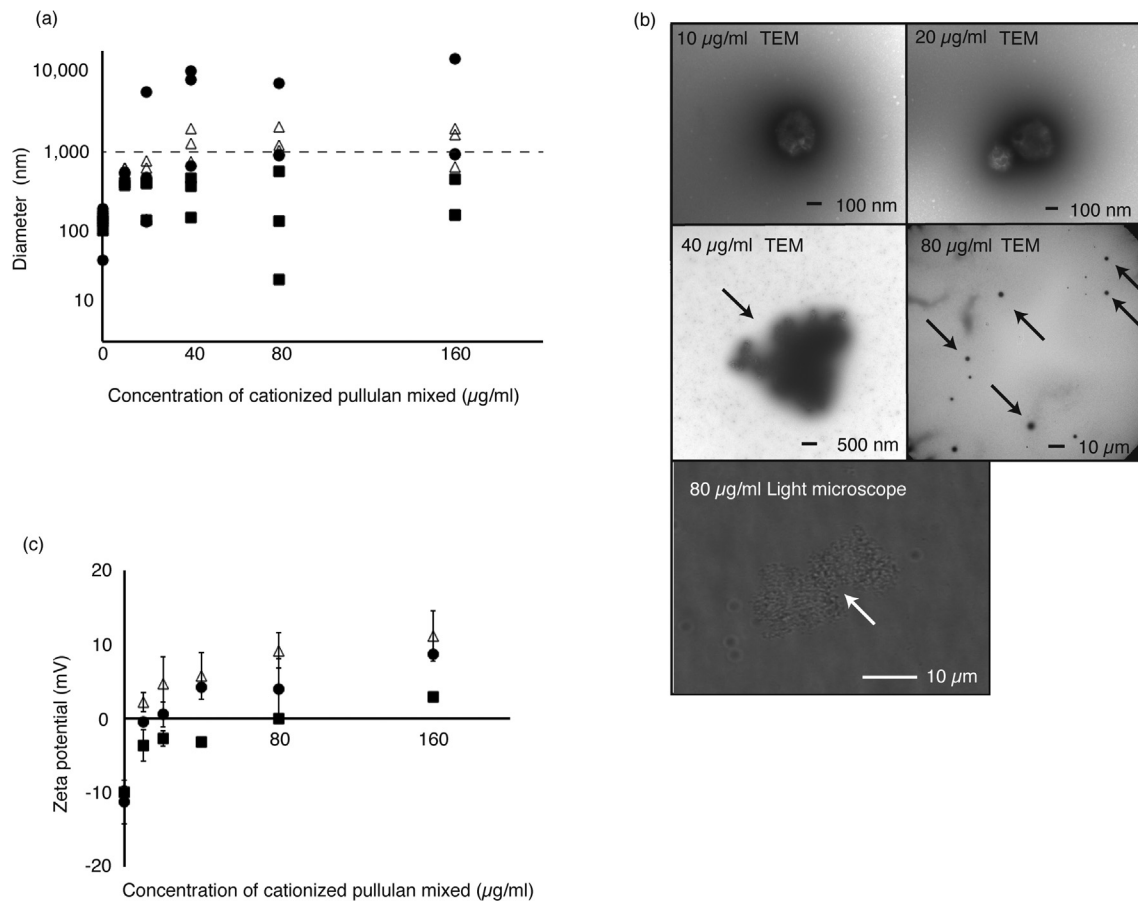
### 3.2. Characterization of exosomes modified with cationized pullulan

Fig. 2 shows the diameter and surface zeta potential of exosomes modified with cationized pullulan. The exosome diameter increased as the increase in the concentrations of cationized pullu-

**Table 2**  
Primers used for quantitative real-time PCR.

mRNA	Forward	Reverse
IL1b	5'-TTCCCCAGGGCATGTTAAGG-3'	5'-TTCTTGTGACCCCTGAGCGAC-3'
IL4	5'-GTAGGGCTTCCAAGTGCTT-3'	5'-GGCATCGAAAAGCCCGAAAG-3'
IL10	5'-CAGAGCCACATGCTCCTAGA-3'	5'-GTCCAGCTGGTCTTGTGTT-3'
HGF	5'-CACCCCTGGGAGTATTGTG-3'	5'-GGGACATCAGTCTCAITCAG-3'
TNF $\alpha$	5'-TCTTCTATTCTGCTTGTGG-3'	5'-GGTCTGGCCATAGAAGTGA-3'
IFN $\gamma$	5'-GGAGGAAGTGGCAAAGGAT-3'	5'-TTCAAGACTTCAAAGTCTGAGG-3'
GAPDH	5'-TGTTGAAGTCACAGGAGACAACCT-3'	5'-AACCTGCCAAGTATGATGACATCA-3'

IL, interleukin; HGF, hepatocyte growth factor; TNF $\alpha$ , tumor necrosis factor- $\alpha$ ; IFN $\gamma$ , interferon- $\gamma$ ; GAPDH, glyceraldehyde-3-phosphate dehydrogenase.



**Fig. 2.** Characterization of exosomes modified with cationized pullulan. Exosomes modified with cationized pullulan into which spermine had been introduced at rates of 6.0 (●), 11.6 (△), and 17.0 (■) mol% were evaluated for their diameter (a), morphological characteristics in representative TEM and light microscope images (b), and surface zeta potential (c).

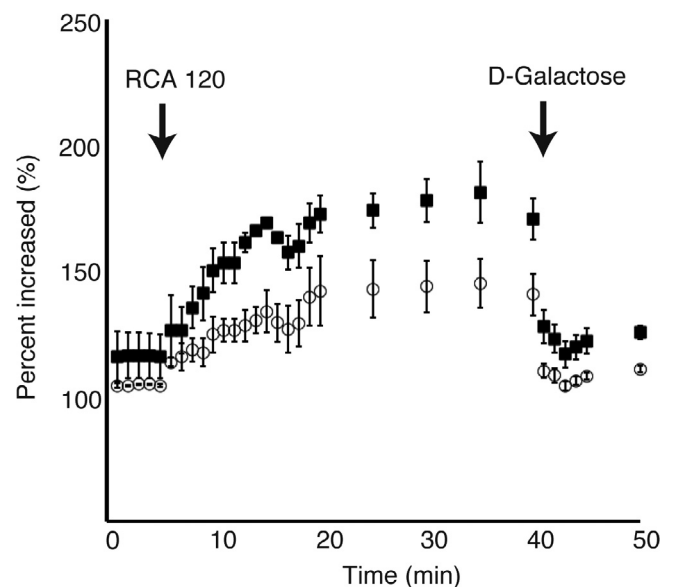
lan reacted. It exceeded 1000 nm at concentration of cationized pullulan of 20 μg/ml or more, and reached approximately 10,000 nm at 40 μg/ml. The aggregation of collected exosomes was observed with a TEM or a light microscope at concentrations of cationized pullulan of 20 μg/ml or more (Fig. 2b, arrow). Before the addition of cationized pullulan, the zeta potential of the original exosomes was approximately -10 mV (Fig. 2c). With an increase in the concentration of cationized pullulan, the zeta potential gradually increased and became positive.

Fig. 3 shows the change of solution turbidity. The turbidity of solution containing exosomes increased with time after the addition of RCA120, but the solution returned to a transparent state after the addition of D-galactose. That indicated the aggregation of exosomes modified with cationized pullulan by the addition of RCA120.

### 3.3. *In vitro* internalization of exosomes modified with cationized pullulan into HepG2 cells

The number of PKH spots in the image was detected as red spots and counted in an automated manner by BZ-X analyzer software (Fig. 4). Sites with a homogeneous HepG2 cell distribution were used for counting to exclude the effect of a difference in the cell number between the images (Fig. 4, the upper images). The beige spots overlapping with red PKH spots were the points detected by the BZ-X analyzer software (Fig. 4, middle and bottom images). Fig. 5 shows the *in vitro* internalization of exosomes modified with cationized pullulan, and its inhibition by the pretreatment of target

cells with a specific receptor inhibitor. Cellular accumulation of PKH was observed as red fluorescent spots, which were located around the CFSE-stained cytoplasm and DAPI-stained nucleus in



**Fig. 3.** Confirmation of the presence of cationized pullulan on the surface of exosomes. Light absorbance induced by the addition of RCA120 to exosomes modified with 10 (○) and 20 (■) μg/ml cationized pullulan is shown.

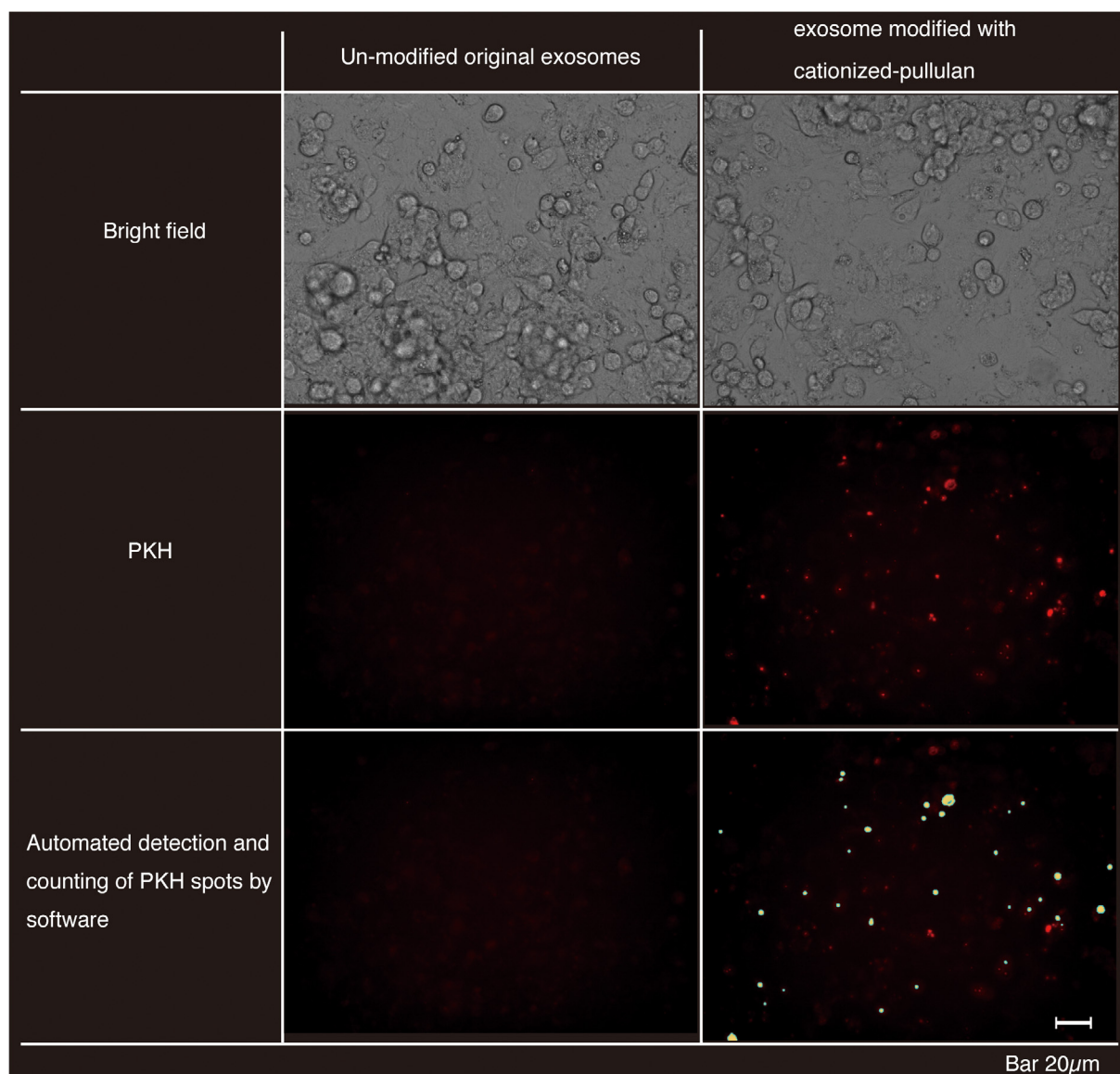


**Fig. 4.** Detection and counting of PKH26 with fluorescent microscope. Sites with a homogeneous HepG2 cell distribution were used for counting to exclude the effect of a difference in the cell number between the images (the upper images). The number of PKH spots in the images was detected in an automated manner by BZ-X analyzer software (middle and bottom images). The beige spots overlapping with PKH26 red spots were the points detected and counted by the BZ-X analyzer software in an automated manner (bottom images).

the group treated with PKH-labeled exosomes modified with cationized pullulan (Fig. 5a). An increased number of PKH spots was observed in the group treated with exosomes modified with cationized pullulan, whereas the original unmodified exosomes were not internalized into HepG2 cells to the same extent as the exosomes modified with cationized pullulan (Fig. 5b). This number increased with the incubation time. After the addition of asialofetuin, the number of PKH spots in the group treated with the exosomes modified with cationized pullulan significantly decreased (Fig. 5c).

#### 3.4. *In vivo* accumulation of exosomes modified with cationized pullulan and their suppressive effects on the mouse liver injury model

Fig. 6 shows the accumulation of PKH, observed *in vivo* as red spots, in a liver specimen from the concanavalin A-induced mouse liver injury model, as well as the distribution in other organs. Colocalization of PKH with the common exosome marker CD81 (Fig. 6a,

yellow circles) was confirmed. PKH was observed at sites with FITC-stained F4/80-positive Kupffer cells in the group that received the original unmodified exosomes (Fig. 6b, blue circles). At the same time, it was observed at more sites besides those at which PKH and F4/80 colocalized (Fig. 6b, white circles) in the group that received exosomes modified with the cationized pullulan. Increases in the number of PKH spots after the modification with cationized pullulan were observed in the liver, lung, and spleen (Fig. 6c). However, a statistically significant increase was observed only in the liver.

Fig. 7 shows the anti-inflammatory effect of exosomes modified with cationized pullulan *in vivo* in the concanavalin A-induced liver injury model. The proportion of necrotic areas in the injured liver was the lowest for the group that received exosomes modified with cationized pullulan, whereas the Ki-67 index was the highest for this group (Fig. 7a and b). Plasma ALT level was significantly suppressed in the same group (Fig. 7c). The mRNA levels of interleukin (IL)-1b, IL-4, and tumor necrosis factor- $\alpha$  (TNF $\alpha$ ) were

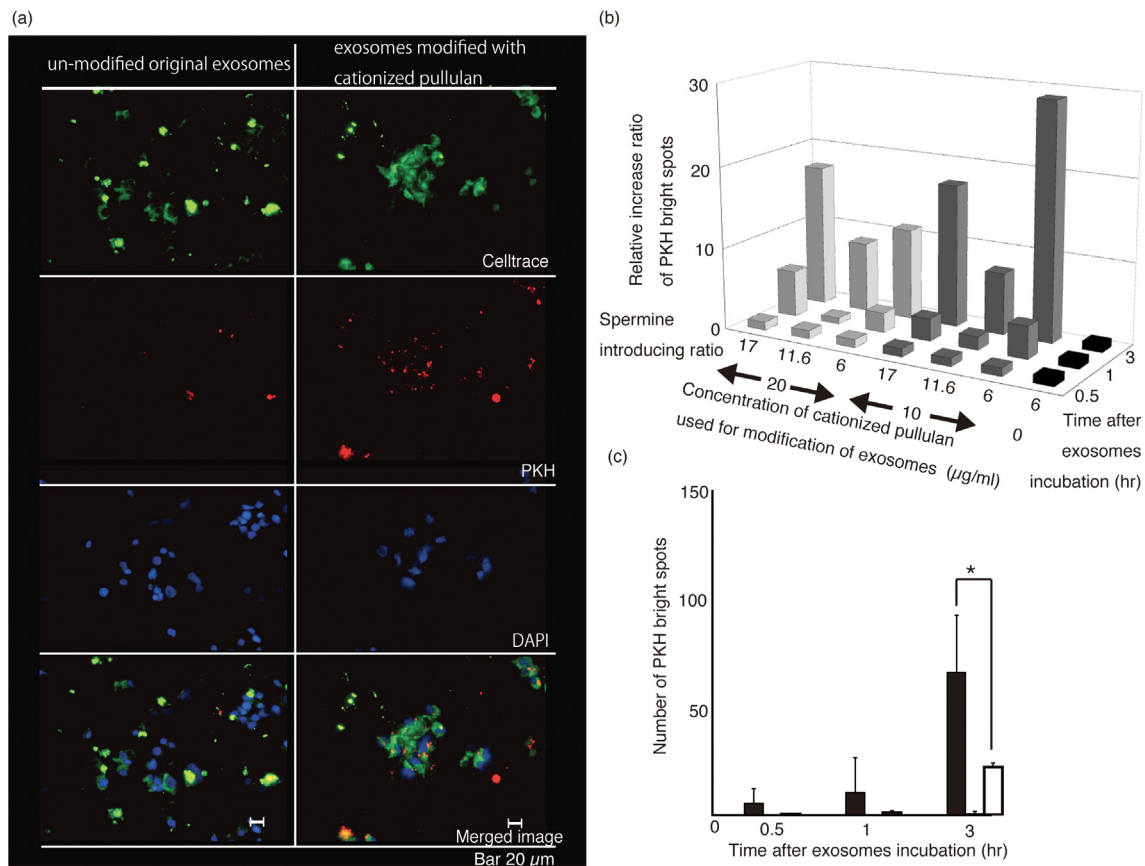


**Fig. 5.** *In vitro* internalization of exosomes unmodified or modified with cationized pullulan into HepG2 cells. (a) Fluorescent microscopic images of HepG2 cells 3 h after incubation with PKH-labeled exosomes. (b) The relative rate of increase in the internalization of PKH as a result of different levels of spermine introduction, concentrations of cationized pullulan, and times of incubation with modified exosomes. The rightmost bar indicates the result of the control group that received PKH26 alone. (c) The number of internalized exosomes with (□) or without (■) ASGPR inhibitor. \* $p < 0.05$ : significant difference between the two groups.

suppressed, whereas those of IL-10 and hepatocyte growth factor (HGF) were enhanced, and the ratio of IL-10 to interferon- $\gamma$  (IFN $\gamma$ ) was higher in the group that received modified exosomes (Fig. 7d). The proportions of Tregs relative to CD4-positive cells among NPCs were increased by treatments with both modified and unmodified exosomes (Fig. 7e). However, the mouse liver injected with modified exosomes showed the most significant increase in the proportion of Tregs.

#### 4. Discussion

The present study demonstrates that the modification of exosomes with cationized pullulan enhanced their accumulation in the injured liver and increased their therapeutic effect. Pullulan is a biomaterial that has a unique property in that it is readily internalized by HepG2 cells or hepatocytes through their galactose-recognized ASGPR [19]. It has been reported that cationized pullulan could make electrostatic interaction with negatively charged substances and work as an efficient liver-targeting carrier for those substances [17,18]. In this study, the chemical introduction of spermine was performed to form a polyionic complex of pullulan and allow the electrostatic interaction with original exosomes with negatively charged surface as schema shown in Fig. S3b [18]. The modification with cationized pullulan could exert several beneficial effects on the enhanced accumulation and therapeutic effect of exosomes on the injured liver.

Exosomes are generally described as extracellular vesicles of less than 100 nm in diameter [30]. Important technical details to

extract exosomes from various materials, including culture supernatants, serum, and other body fluids, were have been described by Théry et al. and the procedures were employed in this study [22]. Furthermore, the extraction methods have been continuously refined to employ newer procedures such as the density gradient ultracentrifugation technique and antibody-dependent collection. A reference regarding such extraction and analysis was published by an international research society [23]. In this study, the majority of collected exosomes ranged from 70 to 100 nm in size, while the remaining fraction was over 100 nm. The mode and mean sizes of collected exosomes were 100 and 125 nm in diameter, respectively (Fig. 1b). The fraction positive for typical surface markers of exosomes, such as CD9 and CD63, was confirmed by flow cytometric analysis (Fig. 1c). Transmission electron microscope images showed the presence of aggregated and single dispersed particles (Fig. S2). Based on the results, particles larger than 100 nm would reflect the presence of aggregated exosomes which was formed through the ultracentrifuge [31]. In this study, collected exosomes were stored at 4 °C and used within 1 week after their purification, even though exosomes are reported to be functionally stable for much longer periods [32,33]. Regarding the functional stability of exosomes, when compared between MSC-derived exosomes and the cells themselves, a similar therapeutic effect has been observed in the *in vivo* mouse injury models [34]. In the previous study, exosomes collected and stored in the same manner as the current study exerted effects on the injured liver model to the same extent as their source MSCs.

In the experiment, the increase of diameter of exosomes by their simple mixing with cationized pullulan could be explained

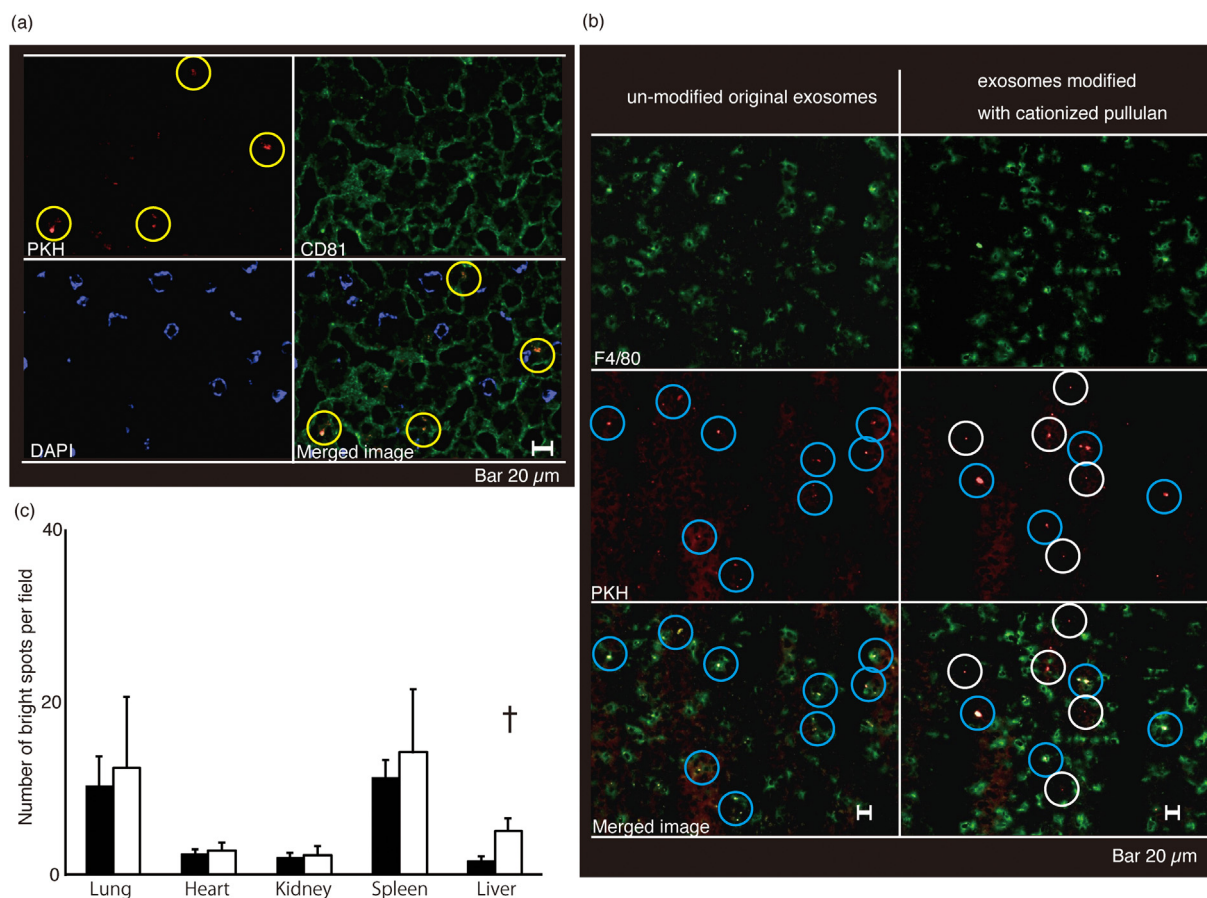


**Fig. 6.** *In vivo* accumulation of unmodified or modified exosomes. (a, b) Presence of PKH in the liver specimen and its colocalization with CD81, a surface marker for exosomes (a), and F4/80-positive Kupffer cells (b) is shown. In Fig. 5b, blue circles indicated the colocalization and non-colocalization of PKH with F4/80-positive cells, respectively. (c) The number of PKH spots in the group that received unmodified (■) or modified PKH-labeled exosomes (□). †p < 0.05: significant difference compared with the group that received original unmodified exosomes. (For interpretation of the references to colour in this figure legend, the reader is referred to the web version of this article.)

by the formation of further exosome aggregates, as observed in TEM images (Fig. 2b). As shown in Fig. 2a, the diameter of the exosomes modified with cationized pullulan at a concentration of 10  $\mu\text{g/ml}$  ranged from 500 to 1000 nm irrespective of the rate of introduction of spermine into the pullulan. The diameter corresponds to the size suitable for caveola-mediated endocytotic pathways [35]. It was reported that exosomes themselves are internalized via clathrin-mediated endocytosis. The endocytotic pathway is for particles with a diameter of less than 200 nm, and particles internalized by cells through this endocytotic pathway are transported into lysosomes, where they are degraded [36,37]. In contrast, particles larger than 500 nm are recognized and internalized via the caveola-mediated endocytotic pathway and thus escape the transport pathway into lysosomes [35]. This difference in cellular pathways would be one of the reasons for the enhanced effect of exosomes modified with cationized pullulan.

The modification with cationized pullulan also affects the surface charge of original exosomes. The modification made the negative surface charge of original exosomes positive (Fig. 2c). The presence of cationized pullulan on the surface of exosomes was evaluated by the aggregative change induced by the addition of lectins recognizable by galactose, and the obtained result clearly indicates the covering of the exosome surface with the added cationized pullulan (Fig. 3). To promote the internalization of nanoparticles by cells, a slightly negative or neutral surface charge is considered to be optimal because an excessive positive charge would cause the nanoparticles to repel each other [38,39]. In this

study, the cationized pullulan into which spermine had been introduced at 6.0 mol%, which is the most weakly cationized pullulan, made the surface charge of exosomes almost neutral at the concentration of 10  $\mu\text{g/ml}$ .

These results would support the reasons why the HepG2 group treated with exosomes modified with cationized pullulan into which 6.0 mol% spermine had been introduced at a concentration of 10  $\mu\text{g/ml}$  showed the most significant relative increase in the number of PKH spots in the *in vitro* study (Fig. 5b).

Most importantly, the modification with cationized pullulan enhanced the process of exosome internalization by HepG2 cells via ASGPR. It is well known that ASGPR is expressed on the surface of hepatocytes and HepG2 cells as well as immature dendritic cells [40–42]. As mentioned before, pullulan is a biomaterial that is readily internalized by HepG2 cells or hepatocytes through their ASGPR, and its high affinity for the liver leads to 80% accumulation of high molecular weight pullulan in the liver [19,43,44]. Several studies have revealed the positive effect of modification with cationized pullulan on *in vivo* liver targeting using the HepG2 cell line [45–47]. As shown in Fig. 5b, the original unmodified exosomes were not internalized into HepG2 cells to the same extent as the exosomes modified with cationized pullulan, whereas PKH internalization was enhanced by pretreatment with the exosomes modified with the cationized pullulan. Concurrently, the influence of an asialoglycoprotein receptor (ASGPR) inhibitor on the cellular uptake was examined to evaluate the contribution of ASGPR to the enhanced internalization of modified exosomes, and the result is

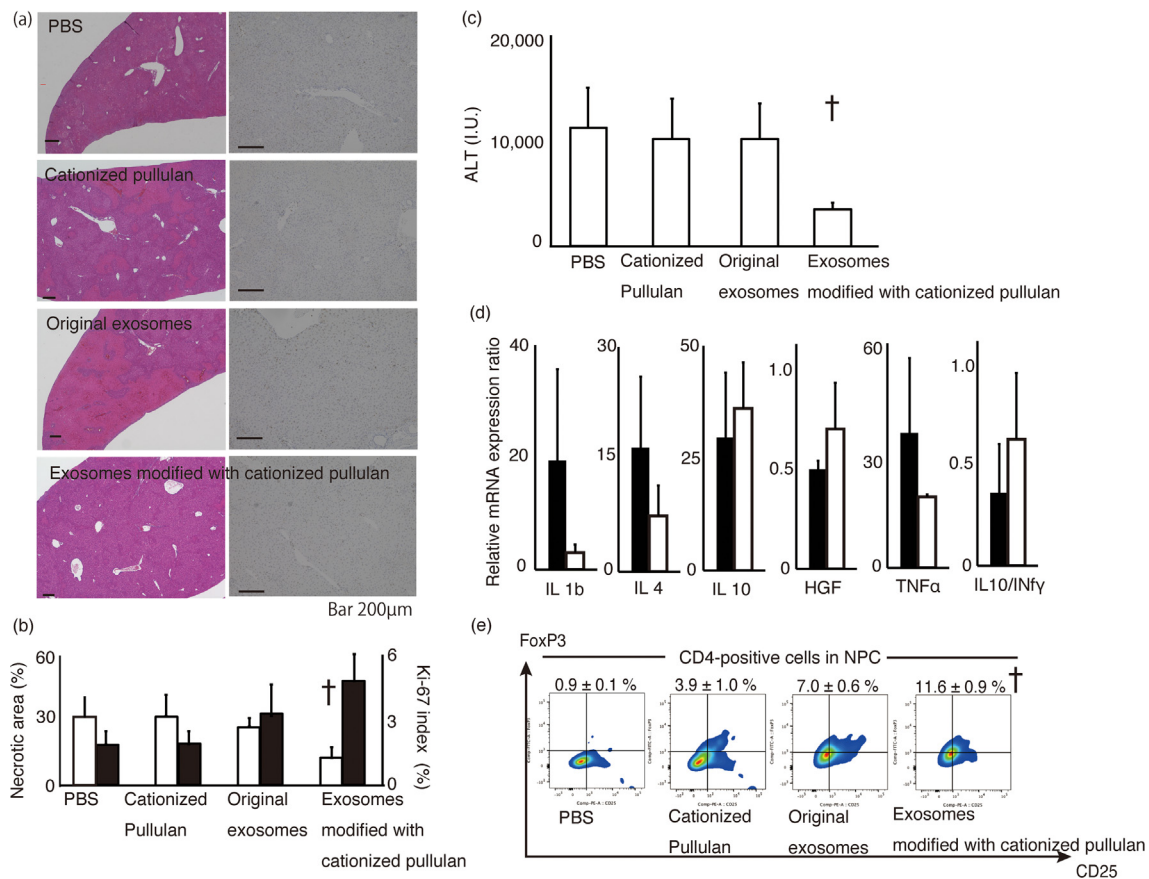


**Fig. 7.** *In vivo* anti-inflammatory effects of unmodified or modified exosomes. (a, b) Liver sample was stained with hematoxylin-eosin (left) and Ki-67 (right) (a), with the proportion of necrotic areas (□) and the Ki-67 index (■) also shown (b). (c) Plasma ALT levels. (d) The mRNA expression levels of cytokines in the group that received unmodified (■) or modified exosomes (□). (e) Flow cytometric analysis of Tregs among CD4-positive cells in NPCs. PBS, cationized pullulan, original unmodified exosomes, and exosomes modified with cationized pullulan in the panel indicating treatment for each mouse group. †p < 0.05: significant difference compared with the group receiving original unmodified exosomes.

described in Fig. 5c. The enhanced internalization of modified exosomes was suppressed by pretreatment of HepG2 cells with asialofetuin. It clearly suggests the involvement of this receptor in the internalization.

Along with the beneficial effect of the modification, however, there is a concern that the covering with the cationized pullulan could cause the alteration of the characteristics of the original exosomes. In this study, the colocalization of PKH and CD81, common surface markers of exosomes, was observed in the liver in the *in vivo* experiment (Fig. 6a). This implies the existence of modified exosomes in the specimen, and may suggest that the modified exosomes still retain their typical surface markers even after being covered with pullulan, even though they have a diameter or positively charged surface that differs from those of the original unmodified exosomes, as shown in Figs. 2 and 3. At the same time, the colocalization of PKH with CD81 would indicate the presence of PKH represented the existence of injected PKH-labeled exosomes with or without modification in the liver. Another concern of cationized pullulan for the modification of exosomes is the possibility of cytotoxicity induced by the cationized pullulan. The cytotoxicity of cationized pullulan has been investigated in previous studies [24,47]. Cytotoxicity was evaluated in HepG2 cells at 5 μg/ml cationized pullulan with 6 mol% introduced spermine. The cell viability was reduced by 20% at 6 h after incubation with the cationized pullulan. The concentration of cationized pullulan used and the incubation time were 5–10-fold higher and 2-fold longer than those in this study. Therefore, it is conceivable that

the cationized pullulan used in this study had a much lower cytotoxic effect.

The effect of modification with cationized pullulan on the accumulation of exosomes in the injured liver was evaluated *in vivo*. The modification of the original exosomes with cationized pullulan increased not only the total number of PKH spots, but also the sites where PKH was observed in the liver. PKH in the mouse group that received the original unmodified exosomes was only observed at the same sites as F4/80-positive cells (Fig. 6b, blue circles), which would indicate that the exosomes had been internalized by Kupffer cells [48]. However, PKH in the mouse group that received exosomes modified with cationized pullulan was observed at additional sites besides where it was colocalized with Kupffer cells (Fig. 6b, white circles). This result implied the presence of different internalization mechanisms other than that involving Kupffer cells, and it would involve a hepatocytic ASGPR-related internalization mechanism for pullulan [19].

The biodistribution of exosomes was evaluated with an *in vivo* imaging system (IVIS) by using 1,1-dioctadecyltetramethyl indotricarbocyanine iodide (DiR)-labeled exosomes (Fig. S4). The DiR dye was mainly observed in the liver and spleen of mice injected with the unmodified or modified DiR-labeled exosomes, while weak signal was observed in the lungs of mice injected with modified exosomes. The result seems to well correspond to that of fluorescent microscopic counting of the number of bright spots shown in Fig. 6c. It is reported that exosomes are generally eliminated from the bloodstream within 2–3 h after the injection and reach the

solid organs, such as liver, lung, and spleen [11,15,49]. The main organ where exosomes are accumulated varies depending on the origin of exosomes employed in the experiment, although the route or dose of injection greatly affects their biodistribution [50].

In this study, a statistically significant increase in the number of PKH spots was observed only in the liver after the administration of modified exosomes (Fig. 6c). This would be derived from the hepatocyte-specific increase in internalization due to the presence of ASGPR on hepatocytes [11].

The enhanced anti-inflammatory and tissue-regenerative effects of modified exosomes were confirmed by the results of plasma ALT level, necrotic area, and Ki-67 index on the concanavalin-A induced liver injury model, and it was compared with the result of treatment with unmodified original exosomes. Concanavalin A injection induces the activation of natural killer cells, an increase in the release of TNF $\alpha$  and IFN $\gamma$ , and the subsequent induction of hepatocyte apoptosis and liver injury, whereas the liver injury can be suppressed through the mechanisms involving Tregs, IL6, and IL10 [51–55]. Kupffer cells play an important role in the initiation of concanavalin A-induced liver injury as well as the induction of tolerance to this liver injury [51,53–55]. The bifunctional nature of Kupffer cells can be explained by the differentiation of macrophages into M1 and M2 phenotypes [56,57]. Exosomes are recognized as one of the most important mechanisms for intercellular signal transmission for macrophages, and it is conceivable that internalization of MSC-derived exosomes by Kupffer cells results in the phenotypic alteration of the cell group and induces an anti-inflammatory effect [14,57,58]. However, the unmodified original exosomes did not show anti-inflammatory effects in this model and it is possible that the anti-inflammatory effect of the unmodified original exosomes might not always produce sufficient therapeutic results based on our results (Fig. 7a–c).

In contrast to the group that received the unmodified original exosomes, the group that received modified exosomes showed an increased number of PKH spots in liver specimens and a significantly enhanced anti-inflammatory effect. This effect was also supported by suppression of the mRNA expression of pro-inflammatory cytokines such as IL1 $\beta$ , IL4, and TNF $\alpha$ , and enhancement of the expression of those with anti-inflammatory or tissue-regenerative effects, such as IL10 and HGF (Fig. 7d). The ratio of IL10 to IFN $\gamma$  increased in the group that received modified exosomes, which would reflect enhancement of the anti-inflammatory mechanism in the liver specimens. Concurrently, the significant increase in the ratio of Tregs to CD4-positive cells among NPCs would also contribute to the anti-inflammatory effect (Fig. 7e). In support of this, it was previously reported the anti-inflammatory change in concanavalin A-induced liver injury was elicited by endogenous prostaglandin I $_2$  and prostaglandin E $_2$  (PGE $_2$ ), which is contained in MSC-derived exosomes, in addition to anti-inflammatory substances such as HGF [59,60].

In this study, the internalization of MSC-derived exosomes by HepG2 cells was enhanced after the modification with cationized pullulan, and the effect was canceled by pretreatment with ASGPR inhibitor. The number of PKH spots increased in the liver specimens, as well as the number of sites of accumulation where it didn't colocalize with Kupffer cells, and eventually, anti-inflammatory effect of MSC-derived exosomes was potentiated. Based on these results, it is possible to say that the modification with cationized pullulan enabled increased accumulation of exosomes specifically into the liver through the direct internalization by hepatocytes via their ASGPR, and it would increase the expression of anti-inflammatory mRNAs and Tregs, resulting in the protective effect in this liver injury model.

## 5. Conclusion

This study is the first to show the accumulation of exosomes in the liver and an enhanced anti-inflammatory effect by the modification of exosomes with cationized pullulan, a well-known biomaterial. It is expected that a combination of biomaterials would confer new targetability on exosomes and improve their *in vivo* functions.

## Appendix A. Supplementary data

Supplementary data associated with this article can be found, in the online version, at <http://dx.doi.org/10.1016/j.actbio.2017.05.013>.

## References

- [1] K. Denzer, M.J. Kleijmeer, H. Heijnen, W. Stoorvogel, H.J. Geuze, Exosome: from internal vesicle of the multivesicular body to intercellular signaling device, *J. Cell Sci.* 113 (19) (2000) 3365–3374.
- [2] H. Valadi, K. Ekström, A. Bossios, M. Sjöstrand, J.J. Lee, J.O. Lötvall, Exosome-mediated transfer of mRNAs and microRNAs is a novel mechanism of genetic exchange between cells, *Nat. Cell Biol.* 9 (6) (2007) 654–659.
- [3] C. Théry, L. Zitvogel, S. Amigorena, Exosomes: composition, biogenesis and function, *Nat. Rev. Immunol.* 2 (8) (2002) 569–579.
- [4] R.C. Lai, F. Arslan, M.M. Lee, N.S.K. Sze, A. Choo, T.S. Chen, M. Salto-Tellez, L. Timmers, C.N. Lee, R.M. El Oakley, Exosome secreted by MSC reduces myocardial ischemia/reperfusion injury, *Stem Cell Res.* 4 (3) (2010) 214–222.
- [5] C. Théry, Exosomes: secreted vesicles and intercellular communications, *F1000 biology reports* 3 (2011) 15.
- [6] C.Y. Tan, R.C. Lai, W. Wong, Y.Y. Dan, S.-K. Lim, H.K. Ho, Mesenchymal stem cell-derived exosomes promote hepatic regeneration in drug-induced liver injury models, *Stem Cell Res. Ther.* 5 (2014) 76.
- [7] H. Pêche, M. Heslan, C. Usal, S. Amigorena, M.C. Cuturi, Presentation of donor major histocompatibility complex antigens by bone marrow dendritic cell-derived exosomes modulates allograft rejection, *Transplantation* 76 (10) (2003) 1503–1510.
- [8] R.C. Lai, T.S. Chen, S.K. Lim, Mesenchymal stem cell exosome: a novel stem cell-based therapy for cardiovascular disease, *Regener. Med.* 6 (4) (2011) 481–492.
- [9] Y. Zhou, H. Xu, W. Xu, B. Wang, H. Wu, Y. Tao, B. Zhang, M. Wang, F. Mao, Y. Yan, Exosomes released by human umbilical cord mesenchymal stem cells protect against cisplatin-induced renal oxidative stress and apoptosis *in vivo* and *in vitro*, *Stem Cell Res. Ther.* 4 (2013) 34.
- [10] S.E. Andaloussi, S. Lakhali, I. Mäger, M.J. Wood, Exosomes for targeted siRNA delivery across biological barriers, *Adv. Drug Deliv. Rev.* 65 (3) (2013) 391–397.
- [11] S.-I. Ohno, M. Takahashi, K. Sudo, S. Ueda, A. Ishikawa, N. Matsuyama, K. Fujita, T. Mizutani, T. Ohgi, T. Ochiya, Systemically injected exosomes targeted to EGFR deliver antitumor microRNA to breast cancer cells, *Mol. Ther.* 21 (1) (2013) 185–191.
- [12] I. Nakase, S. Futaki, Combined treatment with a pH-sensitive fusogenic peptide and cationic lipids achieves enhanced cytosolic delivery of exosomes, *Sci. Rep.* 5 (2015).
- [13] Y. Tabata, Y. Ikada, Effect of the size and surface charge of polymer microspheres on their phagocytosis by macrophage, *Biomaterials* 9 (4) (1988) 356–362.
- [14] C. Lässer, V.S. Alikhani, K. Ekström, M. Eldh, P.T. Paredes, A. Bossios, M. Sjöstrand, S. Gabriellsson, J. Lötvall, H. Valadi, Human saliva, plasma and breast milk exosomes contain RNA: uptake by macrophages, *J. Transl. Med.* 9 (1) (2011) 9.
- [15] Y. Takahashi, M. Nishikawa, H. Shinotsuka, Y. Matsui, S. Ohara, T. Imai, Y. Takakura, Visualization and *in vivo* tracking of the exosomes of murine melanoma B16-BL6 cells in mice after intravenous injection, *J. Biotechnol.* 165 (2) (2013) 77–84.
- [16] S. Yuen, Pullulan and its applications, *Process Biochem.* (1974).
- [17] Y. Tabata, Y. Matsui, K. Uno, Y. Sokawa, Y. Ikada, Simple mixing of IFN with a polysaccharide having high liver affinity enables IFN to target to the liver, *J. Interferon Cytokine Res.* 19 (3) (1999) 287–292.
- [18] J.-I. Jo, M. Yamamoto, K. Matsumoto, T. Nakamura, Y. Tabata, Liver targeting of plasmid DNA with a cationized pullulan for tumor suppression, *J. Nanosci. Nanotechnol.* 6 (9–10) (2006) 2853–2859.
- [19] I. Kanatani, T. Ikai, A. Okazaki, J.-I. Jo, M. Yamamoto, M. Imamura, A. Kanematsu, S. Yamamoto, N. Ito, O. Ogawa, Y. Tabata, Efficient gene transfer by pullulan-spermine occurs through both clathrin- and raft/caveolae-dependent mechanisms, *J. Control. Release* 116 (1) (2006) 75–82.
- [20] J. Jo, M. Yamamoto, A. Okazaki, T. Ikai, Y. Hirano, Y. Tabata, Enhancement of *in vitro* gene transfection efficiency of adult stem cells by cationized polysaccharide derivatives, *Polymer Prepr. Jpn.* 54 (2005) 2142.
- [21] P.A. Knolle, G. Gerken, E. Löser, H.-P. Dienes, F. Gantner, G. Tiegs, K. Meyer zum Büschenfelde, A.W. Lohse, Role of sinusoidal endothelial cells of the liver in

- concanavalin A-induced hepatic injury in mice, *Hepatology* 24 (4) (1996) 824–829.
- [22] C. Théry, S. Amigorena, G. Raposo, A. Clayton, Isolation and characterization of exosomes from cell culture supernatants and biological fluids, *Curr. Protoc. Cell Biol.* (2006) 3.22. 1–3.22. 29.
- [23] A.F. Hill, D.M. Pegtel, U. Lambertz, T. Leonardi, L. O'Driscoll, S. Pluchino, D. Ter-Ovanesyan, E.N. Nolte-t Hoen, ISEV position paper: extracellular vesicle RNA analysis and bioinformatics, *J. Extracellular Vesicles* 2 (2013).
- [24] J. Jo, T. Ikai, A. Okazaki, M. Yamamoto, Y. Hirano, Y. Tabata, Expression profile of plasmid DNA by spermine derivatives of pullulan with different extents of spermine introduced, *J. Controlled Release* 118 (3) (2007) 389–398.
- [25] I. Taniguchi, K. Akiyoshi, J. Sunamoto, Self-aggregate nanoparticles of cholesteryl and galactoside groups-substituted pullulan and their specific binding to galactose specific lectin, RCA120, *Macromol. Chem. Phys.* 200 (6) (1999) 1554–1560.
- [26] J.-I. Jo, A. Okazaki, K. Nagane, M. Yamamoto, Y. Tabata, Preparation of cationized polysaccharides as gene transfection carrier for bone marrow-derived mesenchymal stem cells, *J. Biomater. Sci. Polym. Ed.* 21 (2) (2010) 185–204.
- [27] T. Okamoto, T. Saito, Y. Tabata, S. Uemoto, Immunological tolerance in a mouse model of immune-mediated liver injury induced by 16,16 dimethyl PGE2 and PGE2-containing nanoscale hydrogels, *Biomaterials* 32 (21) (2011) 4925–4935.
- [28] C. Battke, R. Ruiss, U. Welsch, P. Wimberger, S. Lang, S. Jochum, R. Zeidler, Tumour exosomes inhibit binding of tumour-reactive antibodies to tumour cells and reduce ADCC, *Cancer Immunol. Immunother.* 60 (5) (2011) 639–648.
- [29] T. Katsuda, R. Tsuchiya, N. Kosaka, Y. Yoshioka, K. Takagaki, K. Oki, F. Takeshita, Y. Sakai, M. Kuroda, T. Ochiya, Human adipose tissue-derived mesenchymal stem cells secrete functional nephrilysin-bound exosomes, *Sci. Rep.* 3 (2013).
- [30] K.W. Witwer, E.I. Buzas, L.T. Bemis, A. Bora, C. Lasser, J. Lotvall, E.N. Nolte-t Hoen, M.G. Piper, S. Sivaraman, J. Skog, C. Thery, M.H. Wauben, F. Hochberg, Standardization of sample collection, isolation and analysis methods in extracellular vesicle research, *J. Extracellular Vesicles* 2 (2013).
- [31] R. Linares, S. Tan, C. Gounou, N. Arraud, A.R. Brisson, High-speed centrifugation induces aggregation of extracellular vesicles, *J. Extracellular Vesicles* 4 (2015).
- [32] R. Cazzoli, F. Buttitta, M. Di Nicola, S. Malatesta, A. Marchetti, W.N. Rom, H.I. Pass, MicroRNAs derived from circulating exosomes as noninvasive biomarkers for screening and diagnosing lung cancer, *J. Thoracic Oncol.* 8 (9) (2013) 1156–1162.
- [33] H. Kalra, C.G. Adda, M. Liem, C.S. Ang, A. Mechler, R.J. Simpson, M.D. Hulett, S. Mathivanan, Comparative proteomics evaluation of plasma exosome isolation techniques and assessment of the stability of exosomes in normal human blood plasma, *Proteomics* 13 (22) (2013) 3354–3364.
- [34] R. Tamura, S. Uemoto, Y. Tabata, Immunosuppressive effect of mesenchymal stem cell-derived exosomes on a concanavalin A-induced liver injury model, *Inflamm. Regen.* 36 (1) (2016) 26.
- [35] J. Ochieng, V. Furtak, P. Lukyanov, Extracellular functions of galectin-3, *Glycoconj. J.* 19 (7–9) (2002) 527–535.
- [36] J. Rejman, V. Oberle, I. Zuhorn, D. Hoekstra, Size-dependent internalization of particles via the pathways of clathrin- and caveolae-mediated endocytosis, *Biochem. J.* 377 (2004) 159–169.
- [37] T. Tian, Y.L. Zhu, Y.Y. Zhou, G.F. Liang, Y.Y. Wang, F.H. Hu, Z.D. Xiao, Exosome uptake through clathrin-mediated endocytosis and macropinocytosis and mediating miR-21 delivery, *J. Biol. Chem.* 289 (32) (2014) 22258–22267.
- [38] T. Yamaoka, Y. Tabata, Y. Ikada, Blood clearance and organ distribution of intravenously administered polystyrene microspheres of different sizes, *J. Bioactive Compatible Polymers* 8 (3) (1993) 220–235.
- [39] C. He, Y. Hu, L. Yin, C. Tang, C. Yin, Effects of particle size and surface charge on cellular uptake and biodistribution of polymeric nanoparticles, *Biomaterials* 31 (13) (2010) 3657–3666.
- [40] A. Schwartz, S.E. Fridovich, B.B. Knowles, H. Lodish, Characterization of the asialoglycoprotein receptor in a continuous hepatoma line, *J. Biol. Chem.* 256 (17) (1981) 8878–8881.
- [41] V. Kolb-Bachofen, J. Schlepper-Schäfer, W. Vogell, H. Kolb, Electron microscopic evidence for an asialoglycoprotein receptor on Kupffer cells: localization of lectin-mediated endocytosis, *Cell* 29 (3) (1982) 859–866.
- [42] J. Valladeau, V. Duvert-Frances, J.J. Pin, M.J. Kleijmeer, S. Ait-Yahia, O. Ravel, C. Vincent, F. Vega, A. Helms, D. Gorman, S.M. Zurawski, G. Zurawski, J. Ford, S. Saeland, Immature human dendritic cells express asialoglycoprotein receptor isoforms for efficient receptor-mediated endocytosis, *J. Immunol.* 167 (10) (2001) 5767–5774.
- [43] Y. Kaneo, T. Tanaka, T. Nakano, Y. Yamaguchi, Evidence for receptor-mediated hepatic uptake of pullulan in rats, *J. Control. Release* 70 (3) (2001) 365–373.
- [44] T. Yamaoka, Y. Tabata, Y. Ikada, Body distribution profile of polysaccharides after intravenous administration, *Drug Delivery* 1 (1) (1993) 75–82.
- [45] M.R. Rekha, C.P. Sharma, Blood compatibility and in vitro transfection studies on cationically modified pullulan for liver cell targeted gene delivery, *Biomaterials* 30 (34) (2009) 6655–6664.
- [46] M.R. Rekha, C.P. Sharma, Hemocompatible pullulan-polyethyleneimine conjugates for liver cell gene delivery: in vitro evaluation of cellular uptake, intracellular trafficking and transfection efficiency, *Acta Biomater.* 7 (1) (2011) 370–379.
- [47] J.-I. Jo, T. Ikai, A. Okazaki, K. Nagane, M. Yamamoto, Y. Hirano, Y. Tabata, Expression profile of plasmid DNA obtained using spermine derivatives of pullulan with different molecular weights, *J. Biomater. Sci. Polym. Ed.* 18 (7) (2007) 883–899.
- [48] F.L. Willekens, J.M. Werre, J.K. Kruijt, B. Roerdinkholder-Stoelwinder, Y.A. Groenen-Döpp, A.G. van den Bos, G.J. Bosman, T.J. van Berkel, Liver Kupffer cells rapidly remove red blood cell-derived vesicles from the circulation by scavenger receptors, *Blood* 105 (5) (2005) 2141–2145.
- [49] C.P. Lai, O. Mardini, M. Ericsson, S. Prabhakar, C.A. Maguire, J.W. Chen, B.A. Tannous, X.O. Breakefield, Dynamic biodistribution of extracellular vesicles in vivo using a multimodal imaging reporter, *ACS Nano* 8 (1) (2014) 483–494.
- [50] O.P. Wiklander, J.Z. Nordin, A. O'Loughlin, Y. Gustafsson, G. Corso, I. Mager, P. Vader, Y. Lee, H. Sork, Y. Seow, N. Heldring, L. Alvarez-Erviti, C.E. Smith, K. Le Blanc, P. Macchiarini, P. Jungebluth, M.J. Wood, S.E. Andaloussi, Extracellular vesicle in vivo biodistribution is determined by cell source, route of administration and targeting, *J. Extracellular Vesicles* 4 (2015) 26316.
- [51] K. Decker, Biologically active products of stimulated liver macrophages (Kupffer cells), *Eur. J. Biochem.* 192 (2) (1990) 245–261.
- [52] Y. Kaneko, M. Harada, T. Kawano, M. Yamashita, Y. Shibata, F. Gejyo, T. Nakayama, M. Taniguchi, Augmentation of Valpha14 NKT cell-mediated cytotoxicity by interleukin 4 in an autocrine mechanism resulting in the development of concanavalin A-induced hepatitis, *J. Exp. Med.* 191 (1) (2000) 105–114.
- [53] J. Schümann, D. Wolf, A. Pahl, K. Brune, T. Papadopoulos, N. van Rooijen, G. Tiegs, Importance of Kupffer cells for T-cell-dependent liver injury in mice, *Am. J. Pathol.* 157 (5) (2000) 1671–1683.
- [54] A. Erhardt, M. Biburger, T. Papadopoulos, G. Tiegs, IL-10, regulatory T cells, and Kupffer cells mediate tolerance in concanavalin A-induced liver injury in mice, *Hepatology* 45 (2) (2007) 475–485.
- [55] Q. You, L. Cheng, R.M. Kedl, C. Ju, Mechanism of T cell tolerance induction by murine hepatic Kupffer cells, *Hepatology* 48 (3) (2008) 978–990.
- [56] P.J. Murray, T.A. Wynn, Protective and pathogenic functions of macrophage subsets, *Nat. Rev. Immunol.* 11 (11) (2011) 723–737.
- [57] J. Wan, M. Benkdane, F. Teixeira-Clerc, S. Bonnafous, A. Louvet, F. Lafdil, F. Pecker, A. Tran, P. Gual, A. Mallat, M2 Kupffer cells promote M1 Kupffer cell apoptosis: a protective mechanism against alcoholic and nonalcoholic fatty liver disease, *Hepatology* 59 (1) (2014) 130–142.
- [58] B. Zhang, Y. Yin, R.C. Lai, S.S. Tan, A.B. Choo, S.K. Lim, Mesenchymal stem cells secrete immunologically active exosomes, *Stem Cells Dev.* 23 (11) (2014) 1233–1244.
- [59] H. Yin, L. Cheng, R. Langenbach, C. Ju, Prostaglandin I2 and E2 mediate the protective effects of cyclooxygenase-2 in a mouse model of immune-mediated liver injury, *Hepatology* 45 (1) (2007) 159–169.
- [60] M. Record, K. Carayon, M. Poirot, S. Silvente-Poirot, Exosomes as new vesicular lipid transporters involved in cell-cell communication and various pathophysiologicals, *Biochim. Biophys. Acta* 1841 (1) (2014) 108–120.